K+ efflux-independent NLRP3 inflammasome activation by small molecules targeting mitochondria

Christina J. Groß, Ritu Mishra, Katharina S. Schneider, Guillaume Médard, Jennifer Wettmarshausen, Daniela C. Dittlein, Hexin Shi, Oliver Gorka, Paul-Albert Koenig, Stephan Fromm, Giovanni Magnani, Tamara Ćiković, Lara Hartjes, Joachim Smollich, Avril A. B. Robertson, Matthew A. Cooper, Marc Schmidt-Supprian, Michael Schuster, Kate Schroder, Petr Broz, Claudia Traidl-Hoffmann, Bruce Beutler, Bernhard Kuster, Jürgen Ruland, Sabine Schneider, Fabiana Perocchi, Olaf Groß

Angaben zur Veröffentlichung / Publication details:

Groß, Christina J., Ritu Mishra, Katharina S. Schneider, Guillaume Médard, Jennifer Wettmarshausen, Daniela C. Dittlein, Hexin Shi, et al. 2016. "K+ efflux-independent NLRP3 inflammasome activation by small molecules targeting mitochondria." *Immunity* 45 (4): 761–73. https://doi.org/10.1016/j.immuni.2016.08.010.

K^+ Efflux-Independent NLRP3 Inflammasome Activation by Small Molecules Targeting Mitochondria

Christina J. Groß,[1,13] Ritu Mishra,[1,13] Katharina S. Schneider,[1] Guillaume Médard,[2] Jennifer Wettmarshausen,[8] Daniela C. Dittlein,[7] Hexin Shi,[10] Oliver Gorka,[1] Paul-Albert Koenig,[1] Stephan Fromm,[3] Giovanni Magnani,[1] Tamara Ćiković,[1] Lara Hartjes,[1] Joachim Smollich,[1] Avril A.B. Robertson,[11] Matthew A. Cooper,[11] Marc Schmidt-Supprian,[4,5] Michael Schuster,[3] Kate Schroder,[11] Petr Broz,[12] Claudia Traidl-Hoffmann,[7] Bruce Beutler,[10] Bernhard Kuster,[2,9] Jürgen Ruland,[1,5] Sabine Schneider,[6,9] Fabiana Perocchi,[8] and Olaf Groß[1,5,*]

[1]Institut für Klinische Chemie und Pathobiochemie, Klinikum rechts der Isar, Technische Universität München (TUM), 81675 Munich, Germany
[2]Chair of Proteomics and Bioanalytics, TUM, 85354 Freising, Germany
[3]Fachgruppe Analytische Chemie, Department of Chemistry, TUM, 85748 Garching, Germany
[4]Department of Hematology and Oncology, Klinikum rechts der Isar, TUM, 81675 Munich, Germany
[5]TranslaTUM: Zentralinstitut für translationale Krebsforschung, TUM, 81675 Munich, Germany
[6]Department of Chemistry, TUM, 85748 Garching, Germany
[7]Chair and Institute of Environmental Medicine, UNIKA-T, TUM, 86156 Augsburg, and Helmholtz Zentrum München, 85764 Neuherberg, Germany
[8]Genzentrum, Department of Biochemistry, Ludwig-Maximilians-Universität München, 81377 Munich, and Institute of Human Genetics, Helmholtz Zentrum München, 85764 Neuherberg, Germany
[9]Center for Integrated Protein Science Munich (CIPSM), 81377 Munich, Germany
[10]Center for the Genetics of Host Defense, University of Texas Southwestern Medical Center, Dallas, TX 75390, USA
[11]Institute for Molecular Bioscience, The University of Queensland, Brisbane, QLD 4067, Australia
[12]Focal Area Infection Biology, Biozentrum, University of Basel, 4003 Basel, Switzerland
[13]Co-first author
*Correspondence: olaf.gross@tum.de
http://dx.doi.org/10.1016/j.immuni.2016.08.010

SUMMARY

Imiquimod is a small-molecule ligand of Toll-like receptor-7 (TLR7) that is licensed for the treatment of viral infections and cancers of the skin. Imiquimod has TLR7-independent activities that are mechanistically unexplained, including NLRP3 inflammasome activation in myeloid cells and apoptosis induction in cancer cells. We investigated the mechanism of inflammasome activation by imiquimod and the related molecule CL097 and determined that K^+ efflux was dispensable for NLRP3 activation by these compounds. Imiquimod and CL097 inhibited the quinone oxidoreductases NQO2 and mitochondrial Complex I. This induced a burst of reactive oxygen species (ROS) and thiol oxidation, and led to NLRP3 activation via NEK7, a recently identified component of this inflammasome. Metabolic consequences of Complex I inhibition and endolysosomal effects of imiquimod might also contribute to NLRP3 activation. Our results reveal a K^+ efflux-independent mechanism for NLRP3 activation and identify targets of imiquimod that might be clinically relevant.

INTRODUCTION

Inflammasomes are cytoplasmic complexes that control the bioactivity of interleukin-1 (IL-1) family members such as IL-1β by activating the protease caspase-1 (Schroder and Tschopp, 2010). These potent pro-inflammatory cytokines promote protective inflammatory responses in the context of infection, but their dysregulation can lead to pathological inflammation. Although some inflammasomes are triggered by direct binding to pathogen components within the cytoplasm, the NLRP3 inflammasome instead appears to respond to cellular stress signals triggered by structurally diverse pathogens, endogenous danger signals, and environmental irritants (Gross et al., 2011). Despite over a decade of research and overwhelming evidence of a role for NLRP3 in various auto-inflammatory diseases, the precise mechanism of NLRP3 inflammasome activation remains unresolved. A first signal, termed priming, triggers NF-κB-dependent upregulation of NLRP3 and pro-IL-1β expression and also lowers the activation threshold of NLRP3 by additional transcription-independent means (Juliana et al., 2012; Schroder and Tschopp, 2010). Many factors can trigger subsequent NLRP3 activation, including extracellular ATP, potassium (K^+) ionophores, crystals, insoluble particles, and certain pathogens. ROS, K^+ efflux, and endolysosomal leakage drive NLRP3 activation by these diverse agents (Gross et al., 2011). The importance of ROS in NLRP3 activation has been questioned (Muñoz-Planillo et al., 2013), and endolysosomal leakage is selectively involved in NLRP3 activation by particles and crystals (Hornung et al., 2008). In contrast, it is widely accepted that K^+ efflux is a universal requirement for NLRP3 activation (Muñoz-Planillo et al., 2013). NEK7 has been recently identified as a component of the NLRP3 inflammasome, is proposed to sense ROS (Shi et al., 2016) or K^+ efflux (He et al., 2016).

Imiquimod (also known as R837) is a prominent member of a family of small nucleoside-analogs termed imidazoquinolines.

Topical imiquimod formulations obtained FDA approval in 1997 and are a standard therapy for the treatment of superficial skin cancers, actinic keratosis, and genital warts. It was later discovered that imiquimod and the similar molecule R848 (resiquimod) are TLR7 ligands (Hemmi et al., 2002). TLR7 activation mechanistically explains the interferon production and antiviral activity triggered by this class of molecules, and it is classically thought to account for their anti-tumor effect. However, imiquimod also has TLR7-independent effects, such as direct impairment of the growth and survival of cancer cells (Schön et al., 2003), NLRP3 inflammmasome activation in myeloid cells (Kanneganti et al., 2006), and effects on dermal nociceptive neurons (Riol-Blanco et al., 2014), but the underlying molecular mechanism(s) are unknown. These effects of imiquimod might contribute to its antiviral and anti-tumor activity, but also to its adverse effects, including itch, pain, and psoriasis-like inflammation.

The objective of this study was to investigate the mechanism of NLRP3 activation by imiquimod. NLRP3 activation by imiquimod did not require K^+ efflux, but was dependent on ROS and NEK7. We identified the quinone oxidoreductases NQO2 and mitochondrial Complex I as ROS-producing molecular targets of imiquimod. The ROS induced by imiquimod caused rapid oxidation of cysteines in cytoplasmic proteins, which points to a potential mechanism by which ROS signals to NEK7 and NLRP3. Inflammasome activation by imiquimod was greatly impaired by bypass of electron transport through Complex I, revealing a critical role for Complex I dysfunction in NLRP3 activation by imiquimod.

RESULTS

Imiquimod and CL097 Activate NLRP3 to Trigger ASC Oligomerization, IL-1 Secretion, and Pyroptosis

Previous studies have shown that the TLR7 agonist imiquimod can activate the NLRP3 inflammasome (Kanneganti et al., 2006). To determine whether this activity is unique to imiquimod or shared by other TLR agonists, we primed bone-marrow-derived dendritic cells (BMDCs) with lipopolysaccharide (LPS) and then treated with agonists of various other TLRs, and with control inflammasome activators. While all TLR agonists triggered tumor necrosis factor (TNF) secretion from unprimed cells as expected, only imiquimod and the related imidazoquinoline CL097 activated the inflammasome, as indicated by their ability to trigger secretion of IL-1β, IL-1α, and caspase-1 in LPS-primed cells (Figures 1A–1E). The kinetics of IL-1 secretion induced by imiquimod and CL097 were similar to that of ATP and nigericin, which are rapid activators of NLRP3 (Figure 1E). In contrast, R848 from various commercial sources did not activate the inflammasome in LPS-primed BMDCs or bone-marrow-derived macrophages (BMDMs) (Figures 1A–1D, S1A–S1D), despite a superior ability to induce TNF and other NF-κB-dependent cytokines (Figures 1B and 1D) (Hemmi et al., 2002). Other imidazoquinoline and nucleic acid ligands of endosomal TLRs also failed to induce IL-1β secretion (Figures 1A–1D, S1A–S1D). This suggests that TLR7 activation is insufficient for inflammasome activation by imidazoquinolines.

Deficiency of NLRP3 or of the adaptor protein ASC prevented IL-1β cleavage and secretion in response to imiquimod (Figure 1F) (Kanneganti et al., 2006). Imiquimod triggered NLRP3-dependent ASC oligomerization and formation of "specks" (Figures 1G and 1H), and it also triggered pyroptotic release of lactate dehydrogenase (LDH) (Figure 1I). Gasdermin D (GSDMD) is a cleavage target of caspases-1 and -11 that drives pyroptosis and IL-1 secretion in response to inflammasome activators (Kayagaki et al., 2015; Shi et al., 2015). Imiquimod triggered GSDMD cleavage (Figure S1E). GSDMD was dispensable for intracellular IL-1β cleavage but was required for IL-1β secretion in response to imiquimod and other inflammasome activators (Figures 1J and 1K). ASC can recruit caspase-8, which contributes to IL-1β cleavage and secretion after long or strong activation of NLRP3, especially in caspase-1-deficient cells (Sagulenko et al., 2013). Similarly, prolonged stimulation with imiquimod also led to caspase-8 cleavage and minor IL-1β cleavage and secretion in caspase-1- but not ASC-deficient cells (Figure S1F–S1H). Thus, imiquimod triggers the typical effects of NLRP3 activation: ASC oligomerization, caspase recruitment and activation, GSDMD cleavage, IL-1 secretion, and pyroptosis.

We next investigated pathways upstream of NLRP3 that were important for inflammasome activation by imiquimod. LPS priming enhanced caspase-1 cleavage by imiquimod, but it was not absolutely necessary (Figure S2A). IL-1β secretion in response to imiquimod or CL097 was not disrupted by deficiency of purinoreceptor P2RX7, indicating that these molecules do not induce NLRP3 activation indirectly by causing cellular ATP release or by acting as P2RX7 ligands (Figure S2B). Caspase-11 activation by intracellular LPS activates NLRP3 by triggering K^+ efflux (Rühl and Broz, 2015). However, this pathway was not involved in NLRP3 activation in response to imiquimod, because IL-1β secretion was intact in caspase-11-deficient cells (Figure S2C). In myeloid cells, NLRP3 activation by certain triggers might involve apoptotic or necroptotic cell death pathways (Shimada et al., 2012; Vince et al., 2012), and in tumor cells, imiquimod is known to impair growth and survival (Schön et al., 2003). However, we and others observed negligible IL-1α and LDH release and no caspase-3 activation in inflammasome-deficient myeloid cells treated with imiquimod (Figures 1F, 1I, S2D) (Allam et al., 2014). Thus, imiquimod-induced myeloid cell death is a consequence rather than a cause of inflammasome activation. Furthermore, cells lacking the necroptosome protein receptor-interacting protein kinase 3 (RIPK3) or the pro-apoptotic proteins Bax and Bak show no defect in imiquimod-induced inflammasome activation (Allam et al., 2014; Vince et al., 2012), which together with our findings indicates that neither necrotic nor apoptotic death pathways are responsible for the activation of NLRP3 by imiquimod.

Endolysosomal Disruption by Imidazoquinolines Is Not Sufficient for NLRP3 Inflammasome Activation

We confirmed that NLRP3 activation by imiquimod does not rely on TLR7 (Kanneganti et al., 2006), and observed similar results for CL097 (Figures 2A and 2B). However, imiquimod might engage other endosomal receptors aside from TLR7 for NLRP3 activation. Unc93b1 is required for signaling of TLRs 3, 7, 8, 9, and 13 because it regulates the trafficking of these TLRs and other proteins from the endoplasmic reticulum to the endolysosome (Tabeta et al., 2006) (Figure 2C), but Unc93b1 deficiency did not affect IL-1β secretion in response to any NLRP3 activator (Figure 2D). Similarly, endolysosomal acidification is known to be

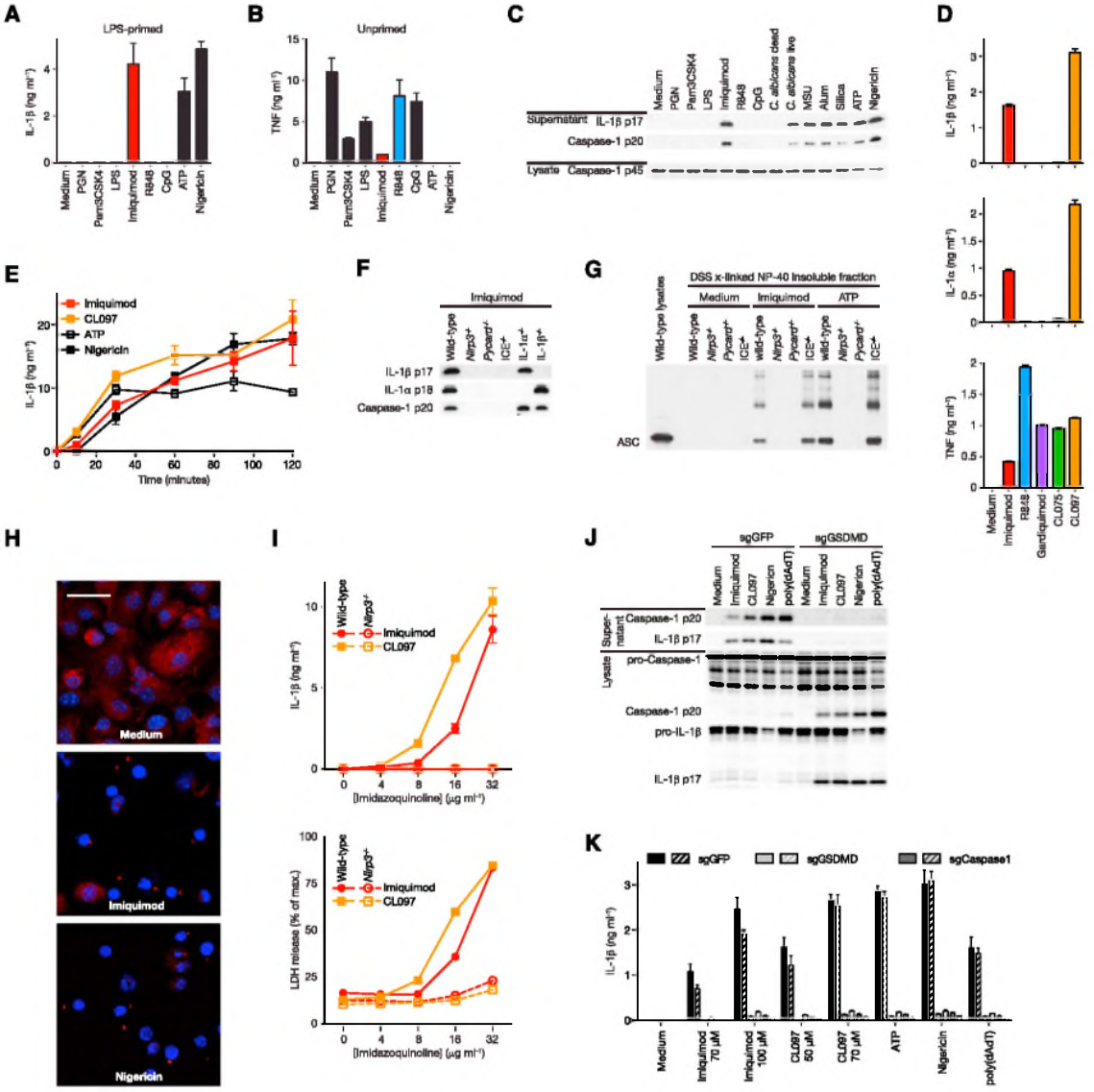

Figure 1. Imiquimod and CL097 Are Unique among TLR Ligands in Activating the NLRP3 Inflammasome

(A and B) BMDCs primed for 3 hr with 20 ng ml^{-1} LPS (A) or left unprimed (B), and then stimulated as indicated. All stimulus concentrations and durations are listed in the Experimental Procedures. IL-1β (A) and TNF (B) were quantified from cell-free supernatants by ELISA.

(C) Immunoblot analysis of lysates and cell-free supernatants from (A).

(D) BMDCs were treated with imidazoquinolines (15 μg ml^{-1}) for 3 hr. IL-1β and IL-1α were measured from supernatant of LPS-primed cells, and TNF from the supernatants of unprimed cells.

(E) Time course of IL-1β secretion from LPS-primed BMDCs treated with 100 μM imiquimod, 70 μM CL097, 5 mM ATP, or 5 μM nigericin.

(F) Immunoblot analysis of supernatants from LPS-primed BMDCs of the indicated genotypes that were treated with 15 μg ml^{-1} of imiquimod for 3 hr.

(G) LPS-primed BMDCs from the indicated mouse strains were treated with imiquimod or ATP. The NP-40-insoluble fraction was enriched by centrifugation, cross-linked with DSS, and analyzed by immunoblotting for monomeric and oligomerized ASC.

(H) Immunofluorescence staining of ASC (red) in LPS-primed BMDCs stimulated with imiquimod or nigericin and then fixed. Nuclei were counterstained with DAPI (blue). Scale bar represents 25 μM.

(I) LPS-primed BMDCs from wild-type or NLRP3-deficient mice were treated with increasing amounts of imiquimod or CL097 for 2 hr. IL-1β (top) and LDH (bottom) were quantified from cell-free supernatants by ELISA and a colorimetric assay, respectively.

(J and K) DCs differentiated from HoxB8-immortalized mouse bone marrow in which *Gsdmd* or *Casp1* were targeted using the CRISPR-Cas9 system were LPS-primed for 3 hr and then stimulated with inflammasome activators. sgRNAs for GFP served as control. (J) Immunoblot analysis of cell-free supernatants and cell lysates. (K) IL-1β was quantified from cell-free supernatants.

Cytokine secretion and LDH release data are depicted as mean ± SEM of technical triplicates. The results from each experiment in this figure are representative of at least three independent experiments. See also Figure S1.

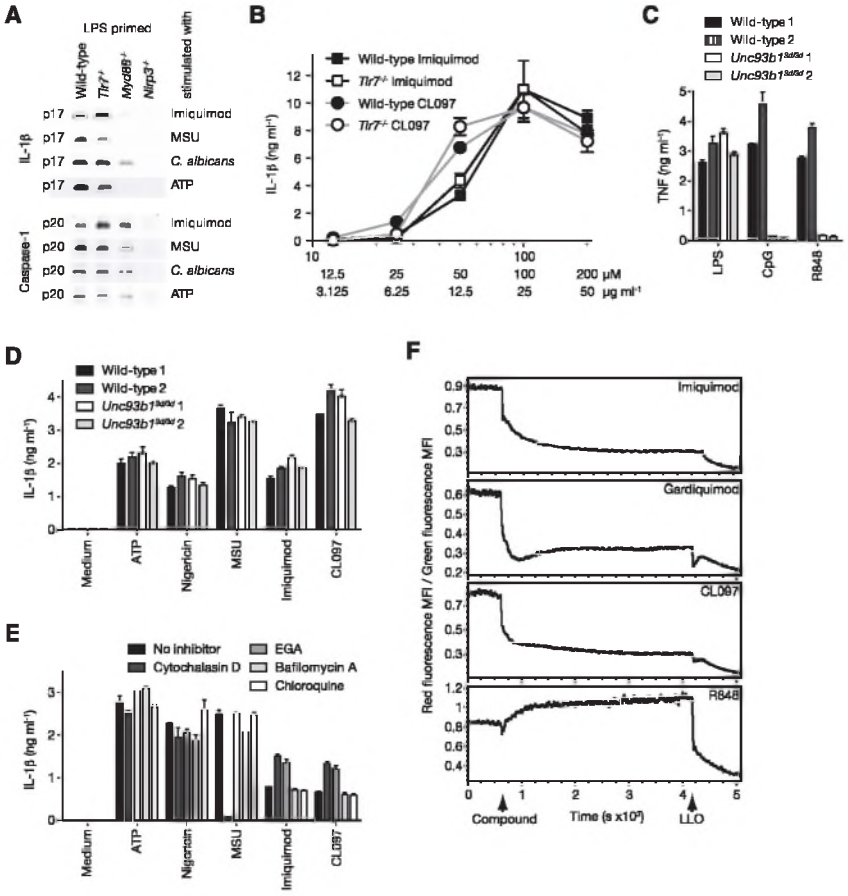

Figure 2. Imidazoquinolines Do Not Require Endosomal TLR Signaling for NLRP3 Activation

(A) LPS-primed BMDCs form the indicated mouse strains were treated with NLRP3 inflammasome activators. Cell-free supernatants were analyzed by immunoblotting.

(B) LPS-primed BMDCs from wild-type and TLR7-deficient mice were treated with the indicated concentrations of imiquimod or CL097 for 3 hr. IL-1β was quantified from cell-free supernatants.

(C and D) BMDCs from wild-type and Unc93b1$^{3d/3d}$ mice were left unprimed (C) or primed with LPS (D) and stimulated as indicated. Cytokines were quantified from cell-free supernatants.

(E) LPS-primed BMDCs were treated with inhibitors of phagocytosis (cytochalasin D), endosomal trafficking (EGA), and lysosomal acidification (bafilomycin A or chloroquine) 30 min prior to addition of the indicated inflammasome activators. IL-1β was quantified from cell-free supernatants.

(F) ASC-deficient BMDMs were labeled with acridine orange, and, subsequently, endolysosomal leakage was analyzed over time by ratiometric measurement of the emission intensities after excitation at 405 nm and 488 nm using a flow cytometer. As a positive control for endolysosomal leakage, LLO was added at the end of each measurement

Cytokine secretion data are depicted as mean ± SEM of technical triplicates. The results from each experiment in this figure are representative of at least two or three separate experiments. See also Figure S2.

important for endosomal TLR signaling but was not required for IL-1β secretion in response to imiquimod, CL097, or other NLRP3 activators (Figures 2E, S2E).

Disruption of the endolysosomal compartment and subsequent leakage of cathepsins into the cytoplasm is implicated in NLRP3 activation by particles and crystals (Hornung et al., 2008). Monosodium urate (MSU) crystals require phagocytosis in order to disrupt the endolysosome and activate NLRP3 (Martinon et al., 2006). In contrast, imiquimod-induced IL-1β secretion was not inhibited by cytochalasin D, an inhibitor of actin polymerization and phagocytosis (Figure 2E). Acridine orange accumulates in the acidic endolysosomal compartment where it fluoresces red, whereas cytoplasmic or nuclear acridine orange fluoresces green. Imiquimod, CL097, and gardiquimod, but not R848, caused a loss of red fluorescence, suggesting that they can induce endolysosomal leakage and/or interfere with endosomal acidification (Figure 2F). While these endolysosomal effects might be involved in NLRP3 activation by imiquimod or CL097, the finding that they are induced by imidazoquinolines that do not activate NLRP3 (i.e., gardiquimod) indicates that they are not sufficient for NLRP3 activation.

K^+ Efflux Is Dispensable for NLRP3 Activation by Imiquimod and CL097

The precise mechanism of NLRP3 activation remains unknown, but a universal requirement for K^+ efflux is now widely accepted. Many studies have shown that preventing K^+ efflux, albeit rather crudely by the use of high extracellular concentrations of KCl, inhibits NLRP3 activation by canonical and non-canonical activators (Muñoz-Planillo et al., 2013; Rühl and Broz, 2015). We were surprised to observe that in BMDCs, caspase-1 and IL-1 cleavage and secretion induced by imiquimod and CL097 were not blocked by extracellular KCl (Figures 3A–3C, S3A). ASC oligomerization in response to imiquimod was similarly resistant to extracellular KCl concentration (Figure 3D). Consistent with the established requirement for K^+ efflux in NLRP3 activation by extracellular ATP, nigericin, MSU, and Candida, IL-1 secretion by these activators was inhibited by increasing concentrations of extracellular KCl. In contrast, the NLRC4 inflammasome activator Salmonella and the AIM2 inflammasome activator intracellular poly(dA:dT) behaved similarly to imiquimod and CL097 in that they triggered cleavage and secretion of caspase-1 and IL-1β even when cells were cultured with extracellular KCl (Figures 3A, 3B, S3A).

The minor but consistent reduction in AIM2 inflammasome activation and LPS-induced TNF secretion suggest that non-physiological K^+ and Cl^- concentrations in the extracellular milieu can influence ASC oligomerization and/or have cellular effects beyond inhibiting K^+ efflux. We therefore examined whether imiquimod induces K^+ efflux. Wild-type or inflammasome-deficient cells were treated with imiquimod, CL097, nigericin, or ATP, and intracellular K^+ concentrations and IL-1β

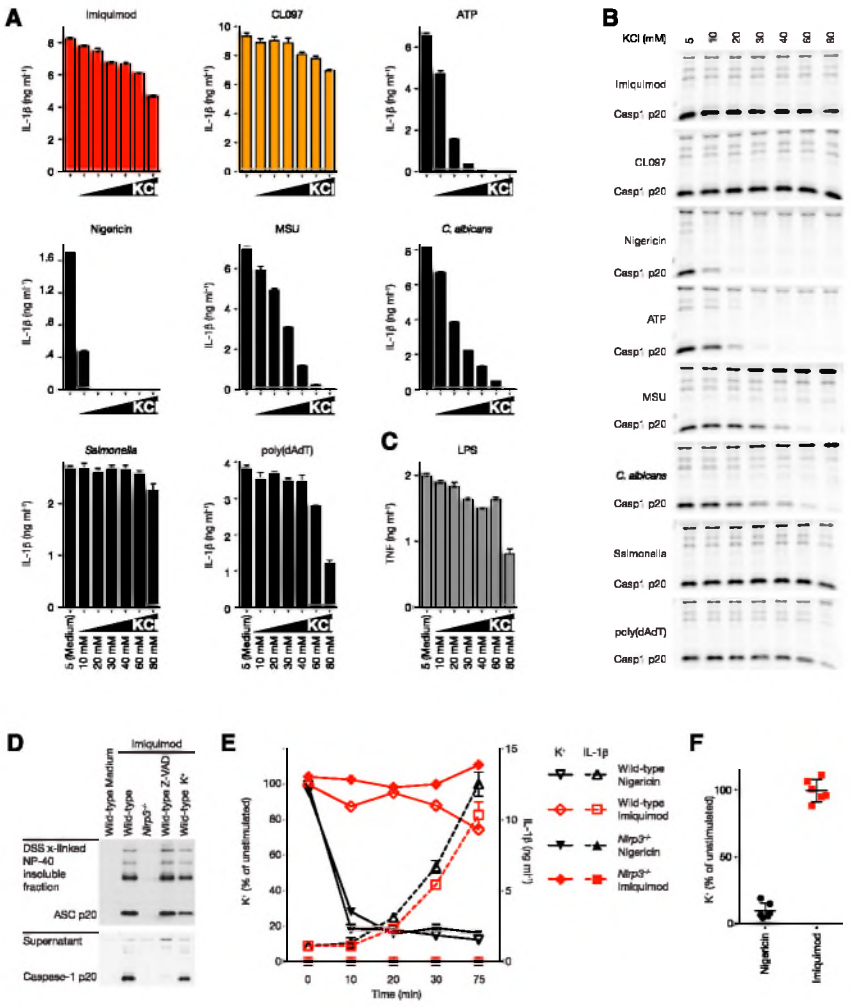

Figure 3. K^+ Efflux-Independent NLRP3 Inflammasome Activation by Imiquimod and CL097

(A) LPS-primed BMDCs were treated with increasing concentrations of extracellular KCl directly before stimulation with the indicated inflammasome activators. IL-1β was quantified from cell-free supernatants.

(B) Immunoblot analysis for caspase-1 in cell-free supernatants from (A).

(C) Unprimed BMDCs were treated with increasing amounts of KCl in parallel to (A) directly before stimulation with 20 ng ml^{-1} LPS for 3 hr. TNF was quantified from cell-free supernatants.

(D) Primed wild-type or NLRP3-deficient BMDCs were pretreated with 20 μM z-VAD-fmk or 50 mM KCl and stimulated with imiquimod. Immunoblot analysis of monomeric and oligomeric ASC in DSS cross-linked NP-40 insoluble fractions (top), and caspase-1 in cell-free supernatants (bottom).

(E) Primed wild-type or NLRP3-deficient BMDCs were treated with nigericin (5 μM) or imiquimod (20 μg ml^{-1}) for the indicated times. IL-1β was quantified from cell-free supernatants (right y axis, dotted lines). Intracellular K^+ concentrations from the same cells were determined by ISE, depicted as percentage of unstimulated cells (right y axis, solid lines).

(F) BMDCs from six different mice were stimulated on separate occasions with nigericin or imiquimod (15-20 μg ml^{-1}) for 30 min and intracellular K^+ concentrations were determined by ISE. Data is depicted as percentage K^+ content of unstimulated cells. Mean ± SD are shown.

Cytokine secretion data are depicted as mean ± SEM of technical triplicates. The results from each experiment in this Figure are representative of at least three independent experiments. See also Figure S3.

secretion were measured. Imiquimod triggered IL-1β secretion in wild-type cells without triggering a loss of cellular K^+ in inflammasome-deficient cells (Figures 3E, 3F, S3B). A minor decrease in cellular K^+ concentrations was observed only at later time points and only in wild-type cells, likely reflecting pyroptotic release of K^+ and other cellular molecules (Fink and Cookson, 2006; Rühl and Broz, 2015). In contrast, nigericin- or ATP-induced IL-1β secretion was preceded by a large and immediate drop in cellular K^+ concentration that was not influenced by inflammasome deficiency (Figures 3E, 3F, S3B). Therefore, K^+ efflux can be a consequence of inflammasome activation but is not required for NLRP3 activation by imiquimod.

ROS Are Required for NLRP3 Activation by Imiquimod and CL097

Considering the lack of a requirement for K^+ efflux in NLRP3 activation by imiquimod and CL097, we asked whether ROS is required for NLRP3 activation by these compounds. NLRP3 activation by imiquimod and CL097 was inhibited by the glutathione peroxidase mimetic ebselen and by pyrrolidine dithiocarbamate (PDTC), neither of which inhibited LPS-induced TNF production, or dsDNA-induced activation of the AIM2 inflammasome (Figures 4A, S4A). Both a cell permeable ethyl ester of glutathione (GSH-EE) as well as N-acetylcysteine (NAC), which increases the cellular glutathione pool, also inhibited NLRP3 activation (Figure S4A), suggesting that ROS-induced NLRP3 activation can be counteracted by thiol-active antioxidants. Indeed, imiquimod and CL097 were potent inducers of general (CellROX), as well as mitochondrial (MitoSOX) ROS (Figures 4C–4E), in inflammasome-deficient cells, demonstrating that ROS provides an upstream signal for NLRP3 activation by these compounds.

These findings suggested that ROS might activate NLRP3 by influencing the oxidation of protein thiol groups. To determine whether ROS induced by imiquimod and CL097 was sufficient to trigger disulfide bond formation, we expressed in macrophages a variant of GFP (roGFP2) that is sensitive to the glutathione redox potential (Waypa et al., 2010), and which can be targeted to the mitochondrial matrix or cytoplasm (Figure S4B). roGFP2 harbors dual cysteines that can be oxidized by ROS to form a disulfide bond, which can be reduced by glutathione. The changes in the oxidation status of roGFP2 leads to a shift in its fluorescence excitation spectrum (Waypa et al., 2010). Imiquimod and CL097 triggered a rapid disulfide bond formation in roGFP2 both in the mitochondria and in the cytoplasm, as

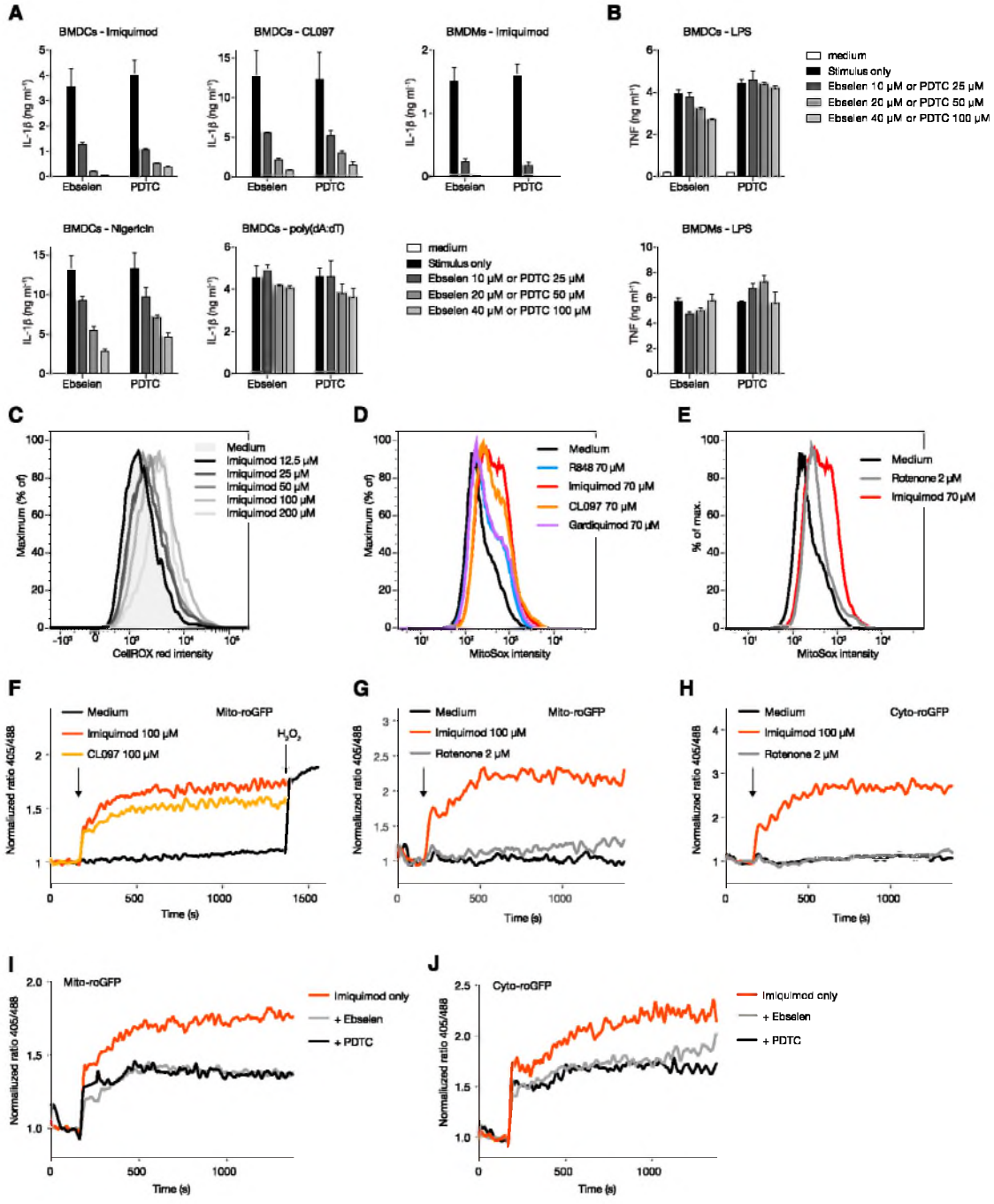

Figure 4. ROS Are Required for NLRP3 Activation by Imiquimod and CL097

(A, B) BMDCs or BMDMs were LPS-primed (A) or left unprimed (B), and treated with increasing doses of Ebselen or PDTC for 30 min and subsequently stimulated as indicated. IL-1β (A) and TNF (B) were quantified from cell-free supernatants.

(C) ASC-deficient BMDMs were labeled with CellROX and then treated with increasing concentrations of imiquimod and analyzed by flow cytometry.

(D and E) ASC-deficient BMDMs were labeled with MitoSOX and then stimulated with imidazoquinolines at 70 µM (D) or with 2 µM rotenone (E) and analyzed by flow cytometry.

(F) BMDMs from expressing the CAR1 adenoviral receptor were transduced with an adenovirus encoding mitochondrial matrix-targeted roGFP2. Fluorescence emission of roGFP2 at 405 nm (oxidized) and at 488 nm (reduced) was measured by flow cytometry and is shown as a ratio. Cells were stimulated with 100 µM Imiquimod or CL097. H_2O_2 served as a positive control for roGFP2 oxidation.

(G) mito-roGFP2-expressing BMDMs as in (F) were treated with 100 µM imiquimod or 2 µM rotenone and analyzed by flow cytometry as in (F).

(H) BMDMs expressing cytoplasmic roGFP2 were stimulated as in (G) and monitored by flow cytometry as in (F).

(legend continued on next page)

determined by the shift in the fluorescence intensity for the two excitation maxima of roGFP2 (405 nm for the oxidized form and 488 nm for the reduced form) (Figures 4F–4H, S4B). Antioxidants that inhibited NLRP3 activation also protected roGFP2 from imiquimod-induced oxidation (Figures 4I and 4J). Therefore, ROS are required for NLRP3 activation by imiquimod and CL097 and might actively signal to NLRP3 by causing the cysteine oxidation of cellular proteins.

The well-established Complex I inhibitor rotenone has been previously reported to activate NLRP3 (Zhou et al., 2011). However, we did not observe NLRP3 activation in response to rotenone, which is in line with several recent studies (Juliana et al., 2012; Muñoz-Planillo et al., 2013; Won et al., 2015) (Figures S4C, S4D, and data not shown). Though rotenone induced mitochondrial ROS, it did not do so as robustly as imiquimod and CL097 (Figure 4E). Rotenone did not induce roGFP2 oxidation, which is in marked contrast to imiquimod and CL097 (Figures 5G and 5H). This suggests that rotenone does not induce sufficient ROS production to oxidize proteins or other macromolecules and thereby fails to activate NLRP3.

Imiquimod and CL097 Target NQO2 and Mitochondrial Complex I

In contrast to other NLRP3 activators, which are either large and complex (e.g., pathogens or particles) and/or which activate NLRP3 by triggering K^+ efflux (e.g., ATP and nigericin), imiquimod and CL097 are small molecules whose mechanism of NLRP3 activation is unique in its independence of K^+ efflux. Additionally, the requirement of ROS for NLRP3 activation by imiquimod and CL097 prompted us to identify protein targets of imiquimod and CL097 that might account for their ability to induce ROS.

We performed chemical proteomics with a bead-coupled imidazoquinoline to identify the targets of imiquimod. Though many proteins from lysates of LPS-primed BMDCs bound to the beads, only the interaction of NQO2 was specific in that binding could be prevented by pre-incubation of BMDC lysates with free imiquimod (Figure 5A). NQO2 is a promiscuous quinone oxidoreductase with unclear physiological function (Vella et al., 2005). NQO2 can produce ROS directly when interacting with certain small molecule inhibitors (Miettinen and Björklund, 2014) and also indirectly via redox cycling of semiquinone radicals (Vella et al., 2005). Indeed, co-crystal structures revealed that imiquimod and CL097 bound the active site of NQO2 and formed an aromatic stack with the isoalloxazine rings of the flavin cofactor (Figures 5B, 5C, S5A–S5F). Interaction of imiquimod and CL097 with NQO2 weakly inhibited its enzymatic activity in an in vitro assay, whereas R848 did not inhibit NQO2 (Figure 5D). The related quinone oxidoreductase NQO1 was not inhibited by imiquimod or CL097 (Figure S5G).

However, NQO2 alone cannot be the only source of ROS induced by imiquimod and CL097, since it is a cytoplasmic protein and we also observed a shift in the mitochondrial redox potential. Furthermore, several established NQO2 inhibitors failed to trigger IL-1β secretion (Figure S5H), indicating that NQO2 inhibition is not sufficient for NLRP3 activation. The electron transport chain is a major source of mitochondrial ROS, and electron transport chain inhibition induces ROS production (Murphy, 2009). To determine whether imiquimod influenced the electron transport chain, we measured the oxygen consumption rate (OCR) in ASC-deficient BMDMs and BMDCs. NLRP3-activating concentrations of imiquimod caused an immediate and dose-dependent decrease in the respiratory rate of both cell types (Figures 5E, 5F, S5I). CL097 also suppressed respiration, but imidazoquinolines that did not activate NLRP3 failed to suppress respiration. Consistent with inhibition of the respiratory chain, imiquimod and CL097, but not R848, caused an immediate reduction in cellular ATP concentrations comparable to the reduction observed with the Complex I inhibitor rotenone or the ATP synthase inhibitor oligomycin A (Figure 5G). Suppression of respiration by imiquimod was observed in a variety of human and murine non-myeloid cell types, indicating that this effect on respiration is not species- or cell type-specific (Figure S5J).

A direct block of the electron transport chain, inhibition of the tricarboxylic acid (TCA) cycle, or general defects in cellular or mitochondrial fitness could account for the suppression of respiration observed with imiquimod. In permeabilized cells, the activity of individual respiratory complexes can be assessed by supplying exogenous TCA cycle intermediates or other electron donors (Salabei et al., 2014). Digitonin-permeabilized BMDMs were incubated with ADP and with substrate combinations to feed Complex I (NADH-linked substrates malate and pyruvate or glutamate), Complex II (succinate, with rotenone), and cytochrome *c*-Complex IV (TMPD with ascorbate). Imiquimod and CL097 selectively blocked Complex I-mediated respiration without affecting respiration via Complex II or via cytochrome *c*-Complex IV, which are downstream of Complex I and Complex II in the respiratory chain (Figure 5H). As observed in intact cells, imidazoquinolines such as R848 and gardiquimod that do not activate NLRP3 also did not influence respiration in permeabilized cells (Figure 5I). Imiquimod also caused an increase in the Complex I substrate NADH, and decreased the NAD^+/NADH ratio (Figure 5J). Collectively, these data suggest that in addition to inhibiting NQO2, imiquimod and CL097 can enter mitochondria, where they are specific inhibitors of another ROS-producing flavoprotein, namely Complex I. Though gardiquimod alone did not trigger NLRP3 activation (Figure 1D), it did influence the endolysosome (Figure 2F) and its combination with separate inhibitors of NQO2 and Complex I did result in IL-1β secretion (Figure S5K). In contrast, dual treatment with NQO2 and Complex I inhibitors did not result in inflammasome activation in the absence of gardiquimod, suggesting that imiquimod activates NLRP3 by simultaneously influencing the endolysosome and ROS-producing flavoproteins or that imiquimod has effects on these or additional proteins that are not fully recapitulated by combining other inhibitors.

Intraperitoneal injection of NLRP3-activating particles, NLRC4-activating bacterial proteins, or the caspase-11 activator LPS

(I and J) BMDMs expressing mito-roGFP2 (I) or cyto-roGFP2 (J) as in (F) were pretreated with 20 μM Ebselen or 100 μM PDTC and then stimulated with 100 μM imiquimod.

Cytokine secretion data are depicted as mean ± SEM of technical triplicates. The results from each experiment in this figure are representative of at least two or three independent experiments. See also Figure S4.

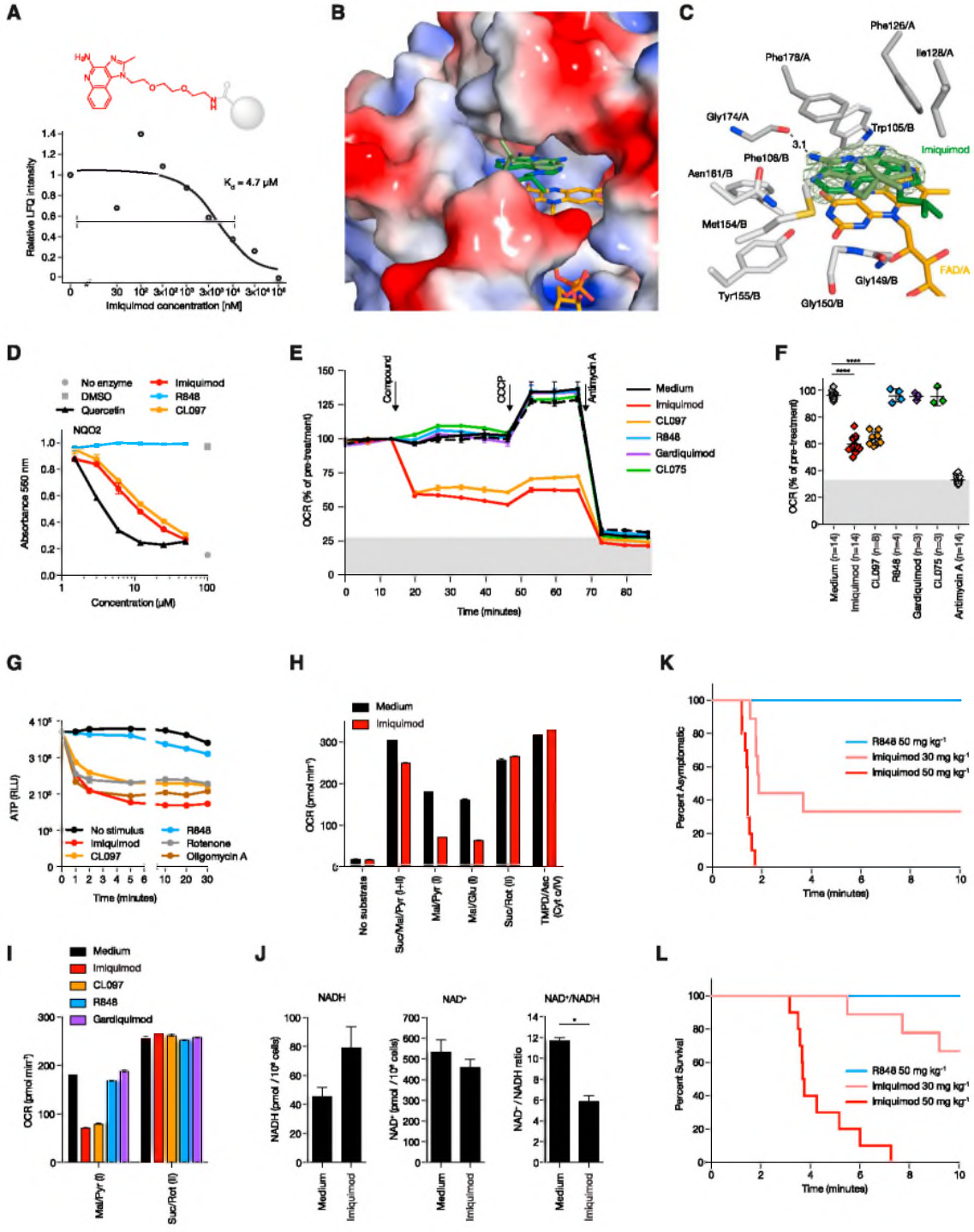

Figure 5. Imiquimod and CL097 Inhibit NQO2 and Complex I

(A) Structure of the imidazoquinoline affinity matrix used for chemical proteomics (top). BMDC lysates were pre-incubated with the indicated concentrations of imiquimod before being applied to the affinity matrix. The LC-MS/MS signal for NQO2 is shown (bottom).

(B) Crystal structure of NQO2 in complex with imiquimod. Surface representation of the active site of NQO2 in complex with imiquimod.

(C) Unbiased Fo-*D*Fc difference density, contoured at 2.5 σ prior to adding imiquimod to the model coordinates. Imiquimod in its two different binding modes and residues of NQO2 lining the active side are shown as stick models. Nitrogens are colored blue, oxygens red, carbon atoms of amino acids gray, the FAD cofactor orange, and imiquimod dark green. Hydrogen bonds are depicted as dashed lines.

(D) Enzymatic activity of recombinant NQO2 in the presence of imidazoquinolines or the control inhibitor quercetin was determined by measuring the absorbance of reduced MTT. Data are representative of three independent experiments.

(legend continued on next page)

represent classic in vivo models for inflammasome-dependent responses. In an attempt to determine whether imiquimod-induced NLRP3 activation was relevant in vivo, we injected imiquimod or R848 i.p. into mice at concentrations similar to what is routinely used for LPS (30–50 mg kg^{-1}, or 0.6–1 mg per 20 g mouse). These high concentrations of systemic imiquimod induced rapid seizures and death (Figures 5K and 5L). This phenotype was not observed at systemic doses of imiquimod below 0.3 mg, consistent with several previous reports (Kanneganti et al., 2006). It cannot be explained by TLR7 activation, for temporal reasons and because R848 did not have the same effect. The finding that the mice succumbed within minutes to systemic imiquimod is an indication that it is not an inflammasome-driven phenotype. Rather, this phenotype is consistent with electron transport chain inhibition and ATP insufficiency in metabolically active cells such as neurons and cardiomyocytes, as is also observed in poisoning with the Complex IV inhibitor cyanide.

Given the implication of mitochondrial ROS in NLRP3 activation and the striking inhibition of Complex I by imiquimod, we asked whether Complex I dysfunction is required for NLRP3 activation by imiquimod. Idebenone and other ubiquinone analogs are used experimentally and clinically to bypass genetic or drug-induced defects in Complex I or downstream electron transport chain complexes (Figure S6A) (Erb et al., 2012; Martinelli et al., 2012). Mechanistically, idebenone delivers electrons into the respiratory chain downstream of Complex I. Idebenone pretreatment rendered cells resistant to the effects of the Complex I inhibitors imiquimod, CL097, and rotenone on respiration (Figures 6A, 6B, S6B–S6D), as expected. Idebenone inhibited NLRP3 activation by imiquimod and CL097 (Figures 6C, S6E), indicating that NLRP3 activation by these compounds involves dysregulated electron transport. In contrast, AIM2 inflammasome activation and LPS-induced TNF secretion was not inhibited by idebenone (Figures 6C and 6D). These data suggest that consequences of Complex I inhibition, such as ROS production and potentially insufficiency of NAD^+ or ATP as well, are necessary for NLRP3 activation by imiquimod.

Imiquimod-Induced NLRP3 Activation Is MCC950-Sensitive and Requires NEK7

The small molecule MCC950 inhibits activation of the NLRP3 inflammasome by activators such as ATP, nigericin, particles, and cytosolic LPS, which all require K^+ efflux for NLRP3 activation (Coll et al., 2015). It is not known how MCC950 prevents NLRP3 activation, but it does not affect K^+ efflux (Coll et al., 2015). MCC950 blocked inflammasome activation by imiquimod, CL097, and other NLRP3 activators, whereas poly(dA:dT)-induced AIM2 inflammasome activation and LPS-induced TNF secretion were unaffected (Figures 7A, 7B, S7A). MCC950 did not prevent imiquimod-induced changes in respiration or roGFP2 oxidation (Figures S7B and S7C).

Recently, NEK7 has been identified as a necessary component of the NLRP3 inflammasome (Shi et al., 2016). Similar to MCC950, NEK7 deficiency does not influence K^+ efflux (He et al., 2016). NEK7 deficiency abrogated NLRP3 activation in response to imiquimod and CL097 (Figures 7C and 7D). In conclusion, imiquimod and CL097 engage a ROS- and Complex I-driven, MCC950-sensitive, NEK7-dependent pathway for NLRP3 activation that is independent of K^+ efflux.

DISCUSSION

K^+ efflux is widely accepted to be a universal requirement for NLRP3 inflammasome activation. Indeed, canonical activation of NLRP3 by ATP, nigericin, and particles (Muñoz-Planillo et al., 2013), as well as non-canonical activation via intracellular LPS and caspase-11 (Rühl and Broz, 2015), requires K^+ efflux for NLRP3 activation. Here we report that imiquimod and CL097 activate NLRP3 independent of K^+ efflux, demonstrating that K^+ efflux is not a universal requirement for NLRP3 activation. Nonetheless, imiquimod induces all the classical downstream effects of NLRP3 activation, including ASC oligomerization, pyroptosis, and secretion of IL-1β.

A role for ROS in NLRP3 activation has been proposed almost a decade ago, but a consensus on the source of ROS and mechanistic data explaining how ROS might activate NLRP3 are lacking. Imiquimod and CL097 are robust inducers of ROS, and activate NLRP3 in a ROS-dependent manner. This led us to postulate that they might have specific protein targets that account for their ability to produce ROS. We identified the flavin-containing quinone oxidoreductases NQO2 and mitochondrial Complex I as molecular targets of imiquimod and CL097. Both NQO2 and Complex I are known to produce ROS as a deleterious byproduct of their normal activity, or when derailed from

(E) Respiration (OCR) of ASC-deficient BMDMs stimulated with imidazoquinolines (75 μM = 21 μg ml^{-1} for imiquimod) and subsequently with CCCP (0.5 μM) and antimycin A (2 μM). The gray area of the graph below the OCR of antimycin A-treated samples indicates the contribution of non-mitochondrial respiration. Data are depicted as mean ± SEM of technical quadruplicates.

(F) OCR of BMDCs and BMDMs treated with 70–75 μM imidazoquinolines or 2 μM antimycin A for 7 min on six separate occasions. Each dot represents a reading (mean of technical quadruplicates) from cells derived from an independent mouse. Mean ± SD of biological replicates is shown. A grouped Student's t test was performed ****$p < 0.0001$.

(G) Cellular ATP concentration (mean ± SEM) of LPS-primed ASC-deficient BMDMs treated with imidazoquinolines (70 μM), oligomycin A (3.5 μM), or rotenone (2 μM) for the indicated times.

(H) OCR of digitonin-permeabilized BMDMs that were given, in the presence or absence of imiquimod (70 μM), ADP, and substrates of the TCA cycle or other electron donors: succinate+malate+pyruvate (Complex I and II), malate+pyruvate (Complex I), malate+glutamate (Complex I), succinate+rotenone (Complex II), or TMPD+ascorbate (cytochrome c-Complex IV). Data are representative of at least three independent experiments.

(I) OCR of digitonin-permeabilized BMDMs that were given, in the presence or absence of imidazoquinolines (70 μM), ADP, and substrates of the TCA cycle or other electron donors as in (H). Data are representative of at least three independent experiments.

(J) Quantification of NAD^+ and NADH from NLRP3-deficient BMDMs treated with imiquimod or left untreated. Pooled results from two independent experiments. *$p = 0.0205$

(K and L) Mice were injected i.p. with the indicated doses of imiquimod or R848 and continuously monitored for onset of convulsions (K) and death (L). Pooled data from three experiments are shown.

See also Figure S5.

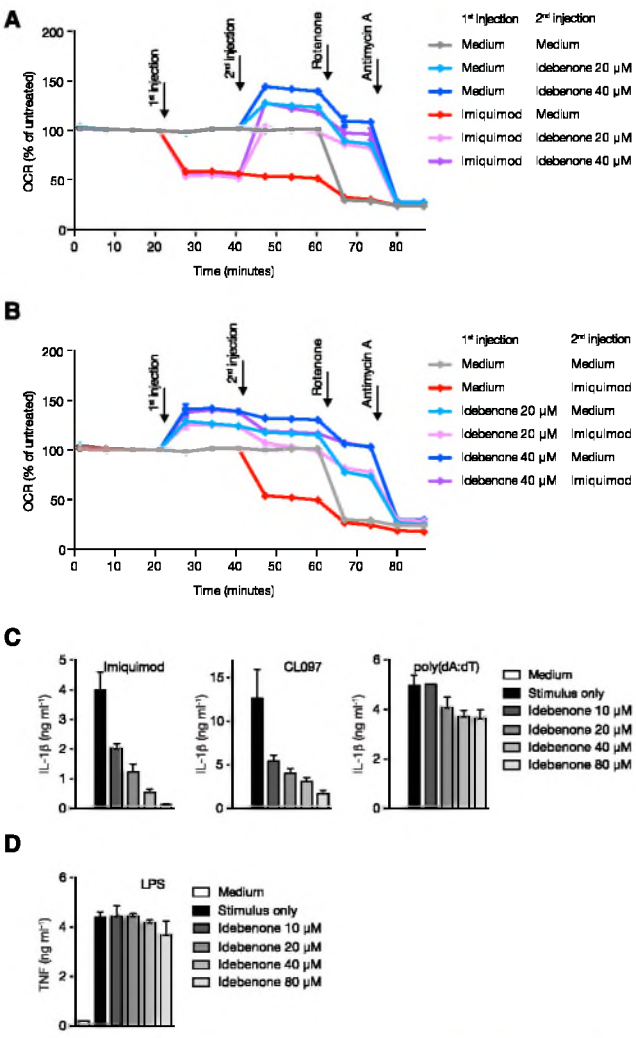

Figure 6. Alleviation of Complex I Dysfunction Inhibits NLRP3 Activation by Imiquimod and CL097

(A and B) OCR of LPS-primed inflammasome-deficient BMDCs, either first treated with Imiquimod (A, first arrow) and subsequently with two different doses of idebenone or first treated with idebenone (B, first arrow) and subsequently with Imiquimod, rotenone (2 µM), and finally with antimycin A (2 µM). (C and D) BMDCs from wild-type mice were LPS-primed (C) or left unprimed (D), and treated with increasing doses of idebenone for 30 min and subsequently stimulated as indicated. Cytokine secretion was determined by ELISA. The results from each experiment in this figure are representative of three independent experiments. See also Figure S6.

their normal function by inhibitors or structural damage (Miettinen and Björklund, 2014; Murphy, 2009; Vella et al., 2005). Electron transfer from reduced flavin cofactors to oxygen is one of the most common mechanisms of protein-mediated ROS generation (Massey, 1994; Murphy, 2009), but redox-cycling of quinones might also be a source of NLRP3-activating ROS induced by imiquimod and CL097. Given the small size of imidazoquinolines and the abundance of cellular flavoproteins, it is possible that imiquimod and CL097 have additional ROS-producing targets that might be involved in NLRP3 activation. Furthermore, endolysosomal effects of imidazoquinolines are not sufficient for NLRP3 activation but might contribute to NLRP3 activation by imiquimod and CL097. However, the observation that rescue of electron transport chain dysfunction also alleviates inflammasome activation demonstrates an important role for Complex I inhibition in NLRP3 activation by imiquimod and CL097.

Antioxidant defenses normally quench ROS and limit its diffusion and chance of reacting with cellular macromolecules (Valko et al., 2007), but our data suggest that imiquimod and CL097 induce ROS robustly enough to overwhelm these defenses and cause rapid oxidation of cysteines in cytoplasmic proteins. In contrast, LPS and rotenone induced only minor mitochondrial ROS and failed to induce cysteine oxidation. Nonetheless, minor mitochondrial ROS production might be an important factor in the ability of LPS and rotenone to acutely reduce the threshold of NLRP3 activation (i.e., to act as priming agents). It has been postulated that NLRP3 must move in close proximity to the mitochondria in order to be activated by mitochondrial ROS (Zhou et al., 2011). However, this might be dispensable for activators such as imiquimod and CL097 that trigger ROS in excess of the threshold for protein oxidation in the cytoplasm.

Our observation that ROS production by NLRP3 activators alters the cysteine oxidation state of cytoplasmic proteins is important because it has been postulated but never demonstrated that ROS-induced cysteine oxidation of a cytoplasmic protein might be a mechanism by which ROS engages signaling pathways for NLRP3 activation. In addition to anti-oxidants, many other inhibitors of NLRP3 activation can modify cysteine residues in proteins (Baldwin et al., 2016). ROS may trigger disulfide bonds in proteins to activate NLRP3, though NLRP3 might also be directly oxidized. For instance, global protein phosphorylation increases rapidly in response to ROS, at least in part because phosphatases are subject to ROS-induced inactivation by oxidation of active site cysteines (Meng et al., 2002). NEK7 has recently been shown to bind NLRP3 and to be necessary for NLRP3 activation by conventional (i.e., K^+ efflux-dependent) activators (He et al., 2016; Shi et al., 2016). We find that NLRP3 activation by imiquimod and CL097 requires NEK7. NEK7 is phosphorylated in a ROS-dependent manner, and dephosphorylation of NEK7 precludes its association with NLRP3 (Shi et al., 2016). Inhibition of phosphatases is one of many possible mechanisms by which ROS induced by imiquimod and other NLRP3 activators might trigger phosphorylation-dependent association of NEK7 and NLRP3.

Pharmacological rescue of electron transport downstream of Complex I by idebenone inhibits NLRP3 activation by imiquimod, demonstrating an important role of Complex I inhibition in NLRP3 activation by imiquimod. In addition to inducing mitochondrial ROS by Complex I inhibition, imiquimod also reduces the NAD^+/NADH ratio and rapidly depletes ATP. These effects of Complex I dysfunction are relieved by idebenone (Erb et al., 2012), suggesting they are important for NLRP3 activation in myeloid cells. The finding that rotenone does not activate NLRP3 indicates that Complex I inhibition is not sufficient for NLRP3 activation in the absence of a robust ROS signal. Nonetheless, it is possible that Complex I defects in vivo might lead to NLRP3-dependent inflammation. Genetic and acquired deficiency in Complex I and other respiratory chain components is associated with inflammation, as seen in some cases of Leigh's syndrome, as well as Alzheimer's disease and Parkinson's

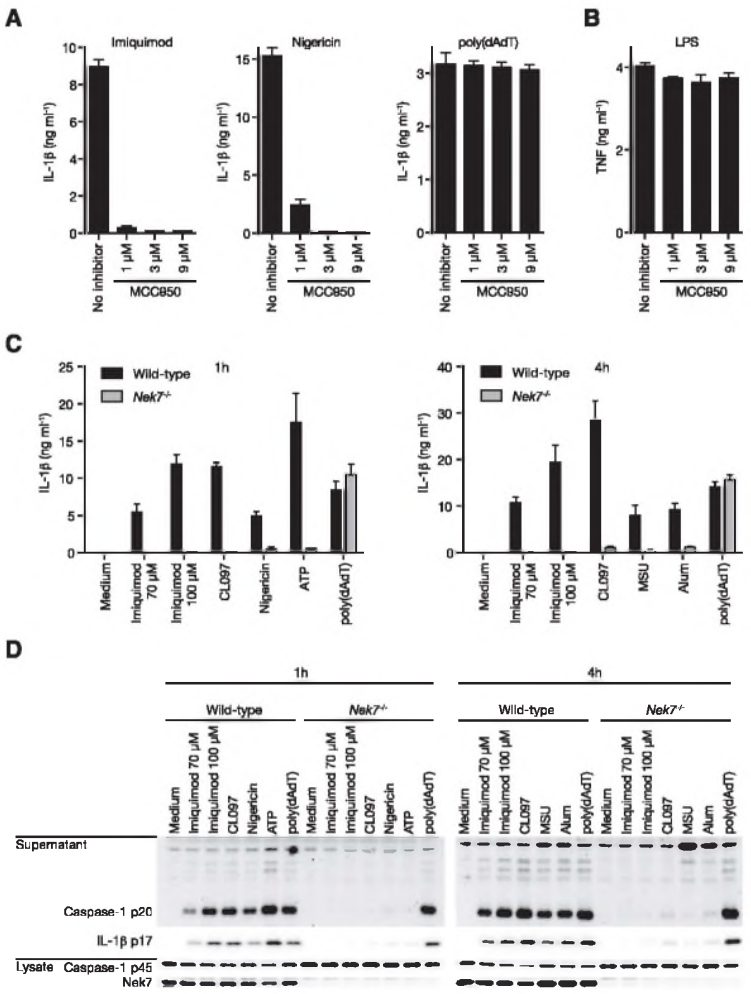

Figure 7. Imiquimod-Induced NLRP3 Activation Requires NEK7 and Is Inhibited by MCC950

(A and B) LPS-primed (A) or unprimed (B) BMDCs were treated with the indicated concentrations of MCC950 30 min prior to stimulation with imiquimod, nigericin, or poly(dA:dT) (A) or LPS (B). Cytokine were quantified from the cell-free supernatant.

(C) LPS-primed BMDCs from wild-type or NEK7-deficient mice were treated with different inflammasome activators, and IL-1β secretion was quantified from the cell-free supernatant.

(D) Immunoblot analysis of cell lysates and cell-free supernatants from (C).

Cytokine secretion data are depicted as mean ± SEM of technical triplicates. The results from each experiment in this figure are representative of at least three independent experiments. See also Figure S7.

disease (Coskun et al., 2012). Complex I activity, and oxidative phosphorylation in general, promote an anti-inflammatory phenotype in myeloid cells and suppresses their pro-inflammatory functions (O'Neill and Hardie, 2013). Macrophages deficient for the Complex I subunit NDUFS4 produce greater amounts of pro-inflammatory cytokines, and this contributes to inflammation observed in the NDUFS4-deficient mouse model of Leigh's syndrome (Jin et al., 2014). These findings raise the possibility that NLRP3 might be involved in inflammation associated with Complex I dysfunction.

Imiquimod is the only FDA-approved imidazoquinoline, and topical imiquimod is the standard treatment for several types of skin cancer. Imiquimod was developed in parallel with R848, and it has been known for many years that in terms of type I IFN production and NF-κB activation in vitro and in vivo, R848 and other imidazoquinolines are up to 100-fold more potent than imiquimod (Hemmi et al., 2002). Our finding that imiquimod inhibits Complex I might explain its direct, TLR7-independent suppression of cancer cell growth and survival (Schön et al., 2003). Despite accumulating evidence for a critical role of Complex I in supporting cancer cell growth and survival (Birsoy et al., 2014; Pollak, 2012), a major concern of using electron transport chain inhibitors as anti-cancer agents is their known toxicity stemming from effects on metabolically active cells. Thus, there is great interest in minimizing the adverse systemic effects of electron transport chain inhibitors, for instance by careful dosing and/or by targeting them to specific tissues (Pollak, 2012; Weinberg and Chandel, 2015). The effects of elevated doses of systemic imiquimod in mice resemble cyanide poisoning, and are consistent with Complex I inhibition and an energetic crisis in metabolically active tissues such as the brain and the heart. It further suggests that a critical component of imiquimod's success and established clinical safety is that topical application maximizes local efficacy and minimizes potentially adverse systemic effects.

EXPERIMENTAL PROCEDURES

Mice

A list of mouse strains used can be found in the Supplemental Information. Housing (SPF or SOPF) and animal experimentation were performed in accordance with European and local guidelines.

Inflammasome Activation and Analysis

BMDCs and BMDMs were generated and stimulated as described in the Supplemental Information (Schneider et al., 2013). Imiquimod, CL097, and other imidazoquinolines (Invivogen) were used at 15–20 μg m^{-1} or 70 μM for 0.5–3 hr. ELISA (eBioscience), immunoblot analysis of cell-free supernatants, cell lysates, and NP-40-insoluble fractions, immunofluorescence imaging of ASC specks, flow cytometric analysis of endolysosomal leakage, and ROS measurements (CellROX and MitoSOX) were performed as described in the Supplemental Information.

CRISPR-Cas9 Mediated Gene Targeting in HoxB8 Cells

ER-HoxB8 immortalized myeloid progenitor cells ("HoxB8 cells") were generated and cultured as described (Wang et al., 2006). pMSCV-Cas9-GFP and pMSCV-sgRNA vectors and retroviral particles were generated and sequentially transduced as described in the Supplemental Information. Cas9- and sgRNA-expressing HoxB8 cells were differentiated for 6–7 days after estrogen withdrawal and treated as described above.

K^+ Measurement

Intracellular K^+ concentrations were determined from cell lysates using an ion-selective electrode (Roche Cobas Analyzer), or by total reflection X-ray fluorescence analysis (Atomika TXRF 8010) as described in the Supplemental Information.

Metabolic Analysis

Oxygen consumption rate (OCR) was measured using a Seahorse XF96 Extracellular Flux Analyzer (Agilent). BMDMs or BMDCs (6–8 × 10^4/well in quadruplicates) were seeded the evening before the experiment. The cells were primed with 50 ng ml^{-1} LPS for 2–3 hr before the medium was changed to bicarbonate- and phenol red-free DMEM 5030 (Sigma) containing 20 ng ml^{-1} recombinant murine M-CSF or GM-CSF, 10 mM glucose, and 2 mM glutamine. Before the assay, the cells were incubated for at least 1 hr at 37°C in a non-CO_2 incubator.

To analyze the activity of individual respiratory chain complexes, we permeabilized BMDMs for 5 min in MAS buffer (220 mM mannitol, 70 mM sucrose, 10 mM KH_2PO_4, 5 mM $MgCl_2$, 2 mM HEPES, 1 mM EGTA, 0.4% fatty acid-free BSA pH 7.2) containing 40 μM digitonin. Digitonin-containing medium was removed and replaced with MAS buffer containing 2 mM ADP and imidazoquinolines in the presence of different combinations of TCA cycle intermediates and electron donors (Salabei et al., 2014).

Intracellular ATP was quantified using the CellTiterGlo Assay (Promega). NAD^+/NADH ratios were measured by enzymatic cycling using the NAD^+/NADH Quantification kit (Biovision).

Measurement of roGFP2 Oxidation

BMDMs from CAR1 transgenic mice (Heger et al., 2015) were transduced with roGFP2-encoding adenovirus (Waypa et al., 2010) as described in the Supplemental Information. The redox status of roGFP2 was expressed by a ratiometric readout of the emission intensities of roGFP2 at 520 nm when exited at 405 or 488 nm.

Chemical Proteomics and NQO2 Biochemistry

An imidazoquinoline affinity matrix was synthesized, and chemical proteomics from BMDC lysates was performed (Médard et al., 2015). Recombinant human NQO2 was bacterially expressed and purified; human NQO1 was from Sigma. Purification and structure determination of NQO2 and enzyme activity assays are described in the Supplemental Information. Structure data can be found at wwPDB under ID 5LBT and 5LBU.

Statistical Analysis

Data were analyzed using a Student's t test. $p < 0.05$ was considered significant.

ACCESSION NUMBERS

Structure data can be found at wwPDB under the IDs PDB: 5LBT, 5LBU.

SUPPLEMENTAL INFORMATION

Supplemental Information includes seven figures, one table, and Supplemental Experimental Procedures and can be found with this article online at http://dx.doi.org/10.1016/j.immuni.2016.08.010.

AUTHOR CONTRIBUTIONS

C.J.G., R.M., K.S.S., G. Médard, J.W., D.C.D., O. Gorka, P.-A.K., S.F., G. Magnani, T.C., J.S., L.H., and O. Groß performed experiments and prepared figures. A.A.B.R., M.A.C., M.S.S., K.S., P.B., H.S., and B.B. generated critical reagents and prepared figures. S.S. performed X-ray crystallography and prepared figures. M.S., C.T.-H., B.K., J.R., and F.P. oversaw a portion of the work. C.J.G. and O. Groß wrote the manuscript, with input from all authors. O. Groß designed and oversaw the research project.

ACKNOWLEDGMENTS

The authors thank Susanne Weiß, Valentin Höfl, Tanja Ruff, Markus Utzt, Michaela Glos, Sandra Reuwand, and Beatrix Lunk for technical assistance, and Stefan Bauer, Hubertus Hochrein, Thomas Korn, Anne Krug, Fiona Müllner, Peter Luppa, Klaus Heger, Tobias Madl, Jean Boutin, and Holger Prokisch for helpful discussions. Thorsten Buch and Philipp Yu provided bone marrow from $TLR7^{-/-}$ and $Unc93b1^{3d/3d}$ mice, respectively. Paul Schumacker provided adenovirus encoding organelle-targeted roGFP2, Laura Trovo and Thomas Misgeld helped setting up the ratiometric ROS measurement, and Deepak Ramanujam and Stefan Engelhardt assisted with adenovirus amplification. The SLS and ESRF provided access and assistance with X-ray crystallography. This work was supported by a postgraduate scholarship from the Natural Sciences and Engineering Research Council of Canada (to C.J.G.), a TUM Graduate School stipend (to K.S.S.), a post-doctoral fellowship of the TUM University Foundation (to P.A.K.), the international doctoral program "i-Target: Immunotargeting in Cancer," funded by the Elite Network of Bavaria (to L.H.), a National Health and Medical Research Council (NHMRC) Project Grant (1086786, to M.A.C. and K.S.), an NHMRC Fellowship (1059354, to AABR), an Australian Research Council Future Fellowship (FT130100361, to K.S.), the Queensland Smart Futures Fund (to K.S.), the Christine Kühne Center for Allergy Research and Education (to C.T.-H.), the Helmholtz Alliance Preclinical Comprehensive Cancer Center (PCCC, to J.R.), the Deutsche Forschungsgemeinschaft (DFG, grants SFB 1054 and RU 695/6-1, to J.R.), the German Cancer Consortium (DKTK, to J.R.), the German Center for Infection Research (DZIF, to J.R.), the DFG and the excellence cluster CIPSM and Fonds der chemischen Industrie (to S.S.), the DFG under the Emmy Noether Programme (PE 2053/1-1, to F.P.), the European Research Council (ERC) under the European Union's Seventh Framework Programme by an ERC Advanced Grant (grant agreement No. 322865, to J.R.) and an ERC Starting Grant (grant agreement No. 337689, to O. Groß), and the Bavarian Ministry of Sciences, Research and the Arts, in the Framework of the Bavarian Molecular Biosystems Research Network (BioSysNet, to O. Groß).

REFERENCES

Allam, R., Lawlor, K.E., Yu, E.C.W., Mildenhall, A.L., Moujalled, D.M., Lewis, R.S., Ke, F., Mason, K.D., White, M.J., Stacey, K.J., et al. (2014). Mitochondrial apoptosis is dispensable for NLRP3 inflammasome activation but non-apoptotic caspase-8 is required for inflammasome priming. EMBO Rep. *15*, 982–990.

Baldwin, A.G., Brough, D., and Freeman, S. (2016). Inhibiting the Inflammasome: A Chemical Perspective. J. Med. Chem. *59*, 1691–1710.

Birsoy, K., Possemato, R., Lorbeer, F.K., Bayraktar, E.C., Thiru, P., Yucel, B., Wang, T., Chen, W.W., Clish, C.B., and Sabatini, D.M. (2014). Metabolic determinants of cancer cell sensitivity to glucose limitation and biguanides. Nature *508*, 108–112.

Coll, R.C., Robertson, A.A.B., Chae, J.J., Higgins, S.C., Muñoz-Planillo, R., Inserra, M.C., Vetter, I., Dungan, L.S., Monks, B.G., Stutz, A., et al. (2015). A small-molecule inhibitor of the NLRP3 inflammasome for the treatment of inflammatory diseases. Nat. Med. *21*, 248–255.

Coskun, P., Wyrembak, J., Schriner, S.E., Chen, H.-W., Marciniack, C., Laferla, F., and Wallace, D.C. (2012). A mitochondrial etiology of Alzheimer and Parkinson disease. Biochim. Biophys. Acta *1820*, 553–564.

Erb, M., Hoffmann-Enger, B., Deppe, H., Soeberdt, M., Haefeli, R.H., Rummey, C., Feurer, A., and Gueven, N. (2012). Features of idebenone and related short-chain quinones that rescue ATP levels under conditions of impaired mitochondrial complex I. PLoS ONE *7*, e36153.

Fink, S.L., and Cookson, B.T. (2006). Caspase-1-dependent pore formation during pyroptosis leads to osmotic lysis of infected host macrophages. Cell. Microbiol. *8*, 1812–1825.

Gross, O., Thomas, C.J., Guarda, G., and Tschopp, J. (2011). The inflammasome: an integrated view. Immunol. Rev. *243*, 136–151.

He, Y., Zeng, M.Y., Yang, D., Motro, B., and Núñez, G. (2016). NEK7 is an essential mediator of NLRP3 activationdownstream of potassium efflux. Nature *530*, 1–16.

Heger, K., Kober, M., Rieß, D., Drees, C., de Vries, I., Bertossi, A., Roers, A., Sixt, M., and Schmidt-Supprian, M. (2015). A novel Cre recombinase reporter mouse strain facilitates selective and efficient infection of primary immune cells with adenoviral vectors. Eur. J. Immunol. *45*, 1614–1620.

Hemmi, H., Kaisho, T., Takeuchi, O., Sato, S., Sanjo, H., Hoshino, K., Horiuchi, T., Tomizawa, H., Takeda, K., and Akira, S. (2002). Small anti-viral compounds activate immune cells via the TLR7 MyD88-dependent signaling pathway. Nat. Immunol. *3*, 196–200.

Hornung, V., Bauernfeind, F., Halle, A., Samstad, E.O., Kono, H., Rock, K.L., Fitzgerald, K.A., and Latz, E. (2008). Silica crystals and aluminum salts activate the NALP3 inflammasome through phagosomal destabilization. Nat. Immunol. *9*, 847–856.

Jin, Z., Wei, W., Yang, M., Du, Y., and Wan, Y. (2014). Mitochondrial complex I activity suppresses inflammation and enhances bone resorption by shifting macrophage-osteoclast polarization. Cell Metab. *20*, 483–498.

Juliana, C., Fernandes-Alnemri, T., Kang, S., Farias, A., Qin, F., and Alnemri, E.S. (2012). Non-transcriptional priming and deubiquitination regulate NLRP3 inflammasome activation. J. Biol. Chem. *287*, 36617–36622.

Kanneganti, T.-D., Ozören, N., Body-Malapel, M., Amer, A., Park, J.-H., Franchi, L., Whitfield, J., Barchet, W., Colonna, M., Vandenabeele, P., et al. (2006). Bacterial RNA and small antiviral compounds activate caspase-1 through cryopyrin/Nalp3. Nature *440*, 233–236.

Kayagaki, N., Stowe, I.B., Lee, B.L., O'Rourke, K., Anderson, K., Warming, S., Cuellar, T., Haley, B., Roose-Girma, M., Phung, Q.T., et al. (2015). Caspase-11 cleaves gasdermin D for non-canonical inflammasome signalling. Nature *526*, 666–671.

Martinelli, D., Catteruccia, M., Piemonte, F., Pastore, A., Tozzi, G., Dionisi-Vici, C., Pontrelli, G., Corsetti, T., Livadiotti, S., Kheifets, V., et al. (2012). EPI-743 reverses the progression of the pediatric mitochondrial disease–genetically defined Leigh Syndrome. Mol. Genet. Metab. *107*, 383–388.

Martinon, F., Pétrilli, V., Mayor, A., Tardivel, A., and Tschopp, J. (2006). Gout-associated uric acid crystals activate the NALP3 inflammasome. Nature *440*, 237–241.

Massey, V. (1994). Activation of molecular oxygen by flavins and flavoproteins. J. Biol. Chem. *269*, 22459–22462.

Médard, G., Pachl, F., Ruprecht, B., Klaeger, S., Heinzlmeir, S., Helm, D., Qiao, H., Ku, X., Wilhelm, M., Kuehne, T., et al. (2015). Optimized chemical proteomics assay for kinase inhibitor profiling. J. Proteome Res. *14*, 1574–1586.

Meng, T.-C., Fukada, T., and Tonks, N.K. (2002). Reversible oxidation and inactivation of protein tyrosine phosphatases in vivo. Mol. Cell *9*, 387–399.

Miettinen, T.P., and Björklund, M. (2014). NQO2 is a reactive oxygen species generating off-target for acetaminophen. Mol. Pharm. *11*, 4395–4404.

Muñoz-Planillo, R., Kuffa, P., Martínez-Colón, G., Smith, B.L., Rajendiran, T.M., and Núñez, G. (2013). K^+ efflux is the common trigger of NLRP3 inflammasome activation by bacterial toxins and particulate matter. Immunity *38*, 1142–1153.

Murphy, M.P. (2009). How mitochondria produce reactive oxygen species. Biochem. J. *417*, 1–13.

O'Neill, L.A.J., and Hardie, D.G. (2013). Metabolism of inflammation limited by AMPK and pseudo-starvation. Nature *493*, 346–355.

Pollak, M.N. (2012). Investigating metformin for cancer prevention and treatment: the end of the beginning. Cancer Discov. *2*, 778–790.

Riol-Blanco, L., Ordovas-Montanes, J., Perro, M., Naval, E., Thiriot, A., Alvarez, D., Paust, S., Wood, J.N., and von Andrian, U.H. (2014). Nociceptive sensory neurons drive interleukin-23-mediated psoriasiform skin inflammation. Nature *510*, 157–161.

Rühl, S., and Broz, P. (2015). Caspase-11 activates a canonical NLRP3 inflammasome by promoting K(+) efflux. Eur. J. Immunol. *45*, 2927–2936.

Sagulenko, V., Thygesen, S.J., Sester, D.P., Idris, A., Cridland, J.A., Vajjhala, P.R., Roberts, T.L., Schroder, K., Vince, J.E., Hill, J.M., et al. (2013). AIM2 and NLRP3 inflammasomes activate both apoptotic and pyroptotic death pathways via ASC. Cell Death Differ. *20*, 1149–1160.

Salabei, J.K., Gibb, A.A., and Hill, B.G. (2014). Comprehensive measurement of respiratory activity in permeabilized cells using extracellular flux analysis. Nat. Protoc. *9*, 421–438.

Schneider, K.S., Thomas, C.J., and Groß, O. (2013). Inflammasome activation and inhibition in primary murine bone marrow-derived cells, and assays for IL-1α, IL-1β, and caspase-1. Methods Mol. Biol. *1040*, 117–135.

Schön, M., Bong, A.B., Drewniok, C., Herz, J., Geilen, C.C., Reifenberger, J., Benninghoff, B., Slade, H.B., Gollnick, H., and Schön, M.P. (2003). Tumor-selective induction of apoptosis and the small-molecule immune response modifier imiquimod. J. Natl. Cancer Inst. *95*, 1138–1149.

Schroder, K., and Tschopp, J. (2010). The inflammasomes. Cell *140*, 821–832.

Shi, J., Zhao, Y., Wang, K., Shi, X., Wang, Y., Huang, H., Zhuang, Y., Cai, T., Wang, F., and Shao, F. (2015). Cleavage of GSDMD by inflammatory caspases determines pyroptotic cell death. Nature *526*, 660–665.

Shi, H., Wang, Y., Li, X., Zhan, X., Tang, M., Fina, M., Su, L., Pratt, D., Bu, C.H., Hildebrand, S., et al. (2016). NLRP3 activation and mitosis are mutually exclusive events coordinated by NEK7, a new inflammasome component. Nat. Immunol. *17*, 250–258.

Shimada, K., Crother, T.R., Karlin, J., Dagvadorj, J., Chiba, N., Chen, S., Ramanujan, V.K., Wolf, A.J., Vergnes, L., Ojcius, D.M., et al. (2012). Oxidized mitochondrial DNA activates the NLRP3 inflammasome during apoptosis. Immunity *36*, 401–414.

Tabeta, K., Hoebe, K., Janssen, E.M., Du, X., Georgel, P., Crozat, K., Mudd, S., Mann, N., Sovath, S., Goode, J., et al. (2006). The Unc93b1 mutation 3d disrupts exogenous antigen presentation and signaling via Toll-like receptors 3, 7 and 9. Nat. Immunol. *7*, 156–164.

Valko, M., Leibfritz, D., Moncol, J., Cronin, M.T.D., Mazur, M., and Telser, J. (2007). Free radicals and antioxidants in normal physiological functions and human disease. Int. J. Biochem. Cell Biol. *39*, 44–84.

Vella, F., Ferry, G., Delagrange, P., and Boutin, J.A. (2005). NRH:quinone reductase 2: an enzyme of surprises and mysteries. Biochem. Pharmacol. *71*, 1–12.

Vince, J.E., Wong, W.W.-L., Gentle, I., Lawlor, K.E., Allam, R., O'Reilly, L., Mason, K., Gross, O., Ma, S., Guarda, G., et al. (2012). Inhibitor of apoptosis proteins limit RIP3 kinase-dependent interleukin-1 activation. Immunity *36*, 215–227.

Wang, G.G., Calvo, K.R., Pasillas, M.P., Sykes, D.B., Häcker, H., and Kamps, M.P. (2006). Quantitative production of macrophages or neutrophils ex vivo using conditional Hoxb8. Nat. Methods *3*, 287–293.

Waypa, G.B., Marks, J.D., Guzy, R., Mungai, P.T., Schriewer, J., Dokic, D., and Schumacker, P.T. (2010). Hypoxia triggers subcellular compartmental redox signaling in vascular smooth muscle cells. Circ. Res. *106*, 526–535.

Weinberg, S.E., and Chandel, N.S. (2015). Targeting mitochondria metabolism for cancer therapy. Nat. Chem. Biol. *11*, 9–15.

Won, J.-H., Park, S., Hong, S., Son, S., and Yu, J.-W. (2015). Rotenone-induced Impairment of Mitochondrial Electron Transport Chain Confers a Selective Priming Signal for NLRP3 Inflammasome Activation. J. Biol. Chem. *290*, 27425–27437.

Zhou, R., Yazdi, A.S., Menu, P., and Tschopp, J. (2011). A role for mitochondria in NLRP3 inflammasome activation. Nature *469*, 221–225.